Oxidation of carbynes: signatures in infrared spectra

Cinquanta, Eugenio; Manini, Nicola ; Ravagnan, Luca; Caramella, Lucia; Onida, Giovanni; Milani, Paolo; Rudolf, Petra

Published in:
Journal of Chemical Physics

DOI:
10.1063/1.4884645

Oxidation of carbynes: Signatures in infrared spectra

E. Cinquanta, N. Manini, L. Ravagnan, L. Caramella, G. Onida, P. Milani, and P. Rudolf

Citation: The Journal of Chemical Physics **140**, 244708 (2014); doi: 10.1063/1.4884645
View online: http://dx.doi.org/10.1063/1.4884645
View Table of Contents: http://scitation.aip.org/content/aip/journal/jcp/140/24?ver=pdfcov
Published by the AIP Publishing

Oxidation of carbynes: Signatures in infrared spectra

E. Cinquanta,[1,2,a),b)] N. Manini,[3,4] L. Ravagnan,[1,4] L. Caramella,[3,4] G. Onida,[3,4] P. Milani,[1,4] and P. Rudolf[5,a)]
[1]*CIMAINA, University of Milan, Via Celoria 16, 20133 Milano, Italy*
[2]*Department of Materials Science, University of Milan Bicocca, Via Cozzi 53, 20125 Milano, Italy*
[3]*European Theoretical Spectroscopy Facility (ETSF), Via Celoria 16, 20133 Milano, Italy*
[4]*Physics Department, University of Milan, Via Celoria 16, 20133 Milano, Italy*
[5]*Zernike Institute for Advanced Materials, University of Groningen, Nijenborgh 4, 9747AG Groningen, The Netherlands*

(Received 9 April 2014; accepted 10 June 2014; published online 30 June 2014)

We report and solidly interpret the infrared spectrum of both pristine and oxidized carbynes embedded in a pure-carbon matrix. The spectra probe separately the effects of oxidation on *sp*- and on sp^2-hybridized carbon, and provide information on the stability of the different structures in an oxidizing atmosphere. The final products are mostly short end-oxidized carbynes anchored with a double bond to sp^2 fragments, plus an oxidized sp^2 amorphous matrix. Our results have important implications for the realization of carbyne-based nano-electronics devices and highlight the active participation of carbynes in astrochemical reactions where they act as carbon source for the promotion of more complex organic species. © *2014 AIP Publishing LLC*. [http://dx.doi.org/10.1063/1.4884645]

I. INTRODUCTION

The allotropes of carbon keep on surprising the scientific community with their extraordinary properties. After fullerenes, nanotubes, and graphene, *sp* carbon (carbyne) is emerging[1] as the building block of novel nanostructured materials, with unexpected features rivaling those of graphene and nanotubes. Promising applications in nanoelectromechanics[2] have been suggested for graphene–carbyne–graphene structures, which display a tunable bandgap[3–5] and a switching behavior induced by conformational changes,[4,6,7] thus realizing pure-carbon logic operators. For these applications to see the day, efficient convenient and fine-tunable production techniques and precise sample characterization methods are needed.

Carbynes of different length and type of termination can now be produced with significant yield thanks to novel synthetic routes and physical strategies.[4,8–14] Carbynes, however, are not as stable in the solid state as sp^2- and sp^3-hybridized carbon. Stabilization strategies have been devised to overcome this problem: the chains can be terminated with bulky stoppers,[15] or anchored to graphene edges[3,16,17] or to sp^2 or sp^3 sites of carbon clusters, or incorporated in an amorphous carbon matrix.[12–14] Using these schemes, individual chains are prevented from coming sufficiently close to each other to react. Although isolating the chains from each other is sufficient to preserve their integrity in Ultra High Vacuum (UHV), exposure to the atmosphere is known to modify *sp*-carbon systems because of the carbynes' high reactivity toward oxygen.[4,12,13] A quantitative characterization of the details and outcomes of this oxidation process is clearly called for. Theoretical predictions foresee that carbynes are turned into shorter chains plus carbon oxides upon reaction with O_2[18,19] but an experimental study under controlled conditions is still lacking. A systematic characterization of carbyne reactivity against oxygen exposure will also impact astrochemistry studies of interstellar dust, where carbynes have been proposed as intermediates in the synthesis of cosmic fullerenes and polyaromatic hydrocarbons.[20,21] Until now, the presence of carbynes in these environments has been difficult to infer because of the lack of reference spectra.[22,23]

In the present paper, we report a systematic experimental and numerical investigation of carbyne reaction with O_2 based on infrared (IR) spectroscopy and *ab initio* simulations.

II. METHODS

Pure *sp*-sp^2 carbon samples were synthesized as clusters inside a pulsed microplasma source[24] using a graphite rod as a target, and deposited at room temperature onto a CaF_2 substrate by a supersonic cluster beam.[25] The deposition rate (∼200 Å/min) was estimated by means of a quartz microbalance, we then set the deposition time in order to obtain a nominal thickness of ∼2 μm. We performed *in situ* IR spectroscopy measurements in transmission mode in UHV conditions (10^{-9} mbar) by using a Brukker IF 66/v FT-IR (Fourier transform infrared) spectrometer, equipped with a liquid-N_2-cooled mercury cadmium telluride detector operating in the range 700–5000 cm^{-1} with a resolution of 2 cm^{-1}. To investigate the reactivity toward oxygen, IR spectra were acquired on a sample deposited in UHV and then exposed to a mixture of 80% He and 20% O_2 at a pressure of 500 mbar for 15 min. After this exposure, the gas mixture was re-evacuated.

We compared the observed spectra with theoretical vibrational frequencies and IR cross sections, computed within density-functional theory in the local spin density

a)Authors to whom correspondence should be addressed. Electronic addresses: eugenio.cinquanta@mdm.imm.cnr.it and p.rudolf@rug.nl
b)Present address: Laboratorio MDM, IMM-CNR, via C. Olivetti 2, I-20864 Agrate Brianza (MB), Italy.

approximation (LSDA) by means of standard density-functional perturbation theory (DFPT) and second-order response to an electric field, as implemented in the Quantum ESPRESSO package.[26,27] Previously, we showed that the vibrational properties of carbynes embedded in an amorphous sp^2 matrix are mainly determined by the end-group geometry.[4] As a model for the pristine material, we thus simulated a carbyne terminated at both sides with zig-zag edge of a graphene nanoribbon, as sketched in the inset of Fig. 2. Core electrons were modelled by ultrasoft pseudopotentials, allowing for a good convergence of the wave-functions/charge density represented in a plane-wave basis with a cutoff of 30/240 Ry (where Ry indicates the Rydberg energy, 13.6 eV). All atomic positions were relaxed until the largest residual force was $<2 \times 10^{-4}$ Ry/a_0 (8 pN). Brillouin-zone integrations of metallic systems were performed using a 2×10^{-4} Ry-wide Gaussian smearing of the electronic-state occupancies. We adopted simulation supercells involving three hexagonal units along the periodic direction, and left at least 7 Å of vacuum separating periodic images in the two other directions, optimizing the lattice constant until the stress tensor dropped below 2×10^{-5} Ry/a_0^3 (0.3 GPa). We sampled the Brillouin zone with at least 13 k-points in each periodic direction and only $k = 0$ components in non-periodic directions. As a model for the oxidized material, we simulated a carbyne terminated at one end with the zig-zag edge of a graphene nanoribbon and at the other end with an oxygen atom.

The systematic mismatch between the observed and simulated vibrational frequencies is to be attributed to the well-known[27] tendency of the LSDA to overestimate (by ∼20%) the cohesive energies and underestimate the bond lengths of molecules and solids, thus leading to slightly overestimated vibrational frequencies (∼1%).

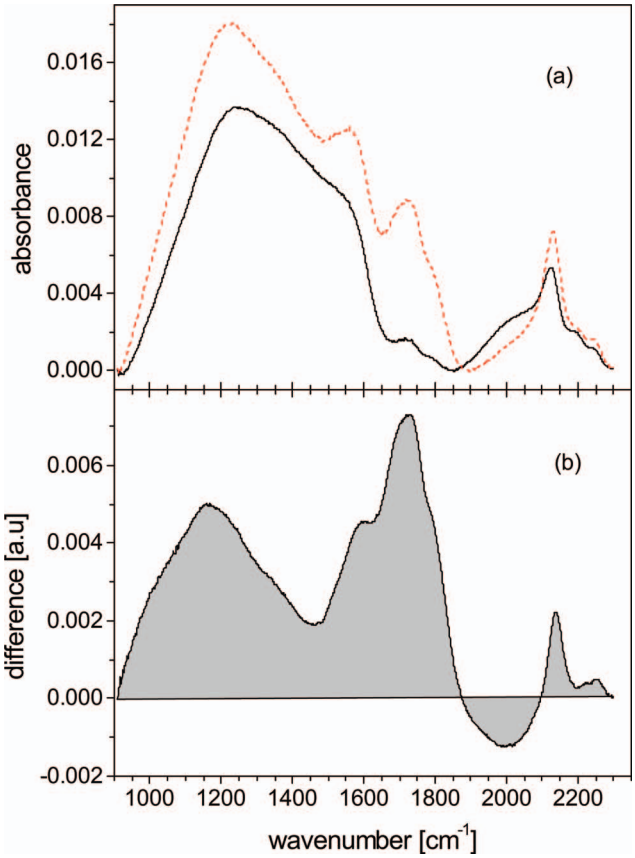

FIG. 1. (a) The IR spectrum of a pure carbon film composed of a sp^2 or sp^3 hybridized amorphous matrix (mainly responsible for the broad spectral feature on the left) containing bonded carbynes whose stretching modes produce the spectral features above 1850 cm^{-1}. Solid line: the pristine pure carbon film; dashed line: spectrum taken after exposure to 500 mbar of He-O_2 (for details see text). (b) The difference spectrum highlighting the spectral features associated with oxidized species.

III. RESULTS

Our experimental data, shown in Fig. 1(a), represent the first identification of the coexistence of sp and sp^2 hybridization in a pure-carbon material based only on IR spectroscopy. The prominent broadband at 1000–1600 cm^{-1} is mainly due to sp^2 carbon, encompassing both the antisymmetric C=C stretching vibrations of graphitic (∼1590 cm^{-1}) and amorphous (∼1360 cm^{-1}) domains,[28,29] while the well-separated structure in the 1900–2300 cm^{-1} range is attributed to the IR-active stretching modes of carbynes. As illustrated in Fig. 2, the IR band of sp carbon is characterized by three sharp components between 2150 and 2300 cm^{-1}, plus a broad unresolved shoulder between 1900 and 2100 cm^{-1} (see the Appendix for details about the fitting procedure). The frequency of the most intense IR feature (the "IR-α" mode, in analogy with R-α mode of Raman spectroscopy[30,31]) in this region is predicted to depend on the chain termination and on the chemical nature of the ligands, as shown by systematic analysis of the vibrational spectra of end-capped carbynes.[30,31] However, in contrast and at complete variance with the Raman-active modes, the carbyne length has little effect on the IR-α frequency but strongly affects the absorption strength. Consequently, the simultaneous presence of carbynes of different

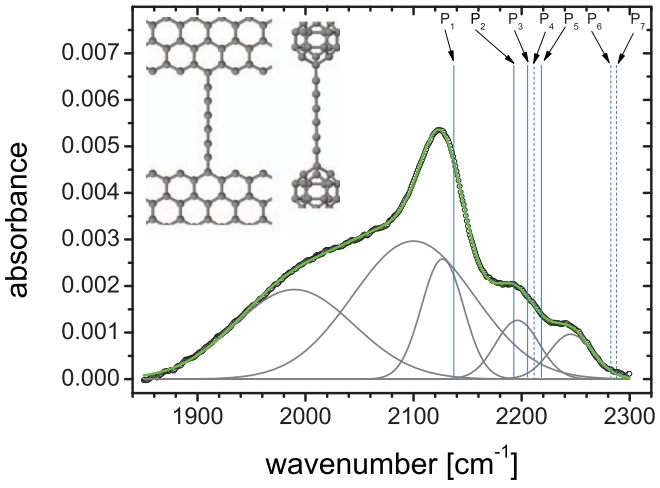

FIG. 2. Open circles: detail of the region of the stretching modes of carbynes of the IR spectrum of Fig. 1 collected on the pristine sample, decomposed into a sum of Gaussian peaks (grey lines), as described in the Appendix. Vertical solid and dashed lines represent the computed frequencies of sp^2- and sp^3-terminated C_n ($n = 4$–10) carbynes, respectively. For the assignment of P1-P7 see text. Inset: models adopted for the simulations of C_6 carbynes bonded to sp^2 and sp^3 hybridized terminations.

TABLE I. The computed frequencies of the most intense IR-active (IR-α) vibrational modes for sp^2- and sp^3-terminated carbynes in a pure carbon matrix. NR stands for graphene nanoribbon.

Model	IR-α (cm^{-1})	Label in Fig. 2
NR-C_4-NR	2138	P1
NR-C_6-NR	2214	P2
NR-C_8-NR	2206	P4
NR-C_{10}-NR	2195	P5
C_{20}-C_4-C_{20}	2211	P3
C_{20}-C_6-C_{20}	2282	P6
C_{20}-C_8-C_{20}	2287	P7

lengths in the sample does not prevent us from identifying and predicting a clustering of the IR vibrational frequencies due to carbynes into distinct groups, associated with the different ligands involved.

In detail, Fig. 2 shows a comparison between the observed spectrum and the computed *ab initio* theoretical results for the IR-α modes of carbynes of different chains lengths, terminated with either sp^2- or sp^3-hybridized C, summarized in Table I.

Apart from the aforementioned shift induced by LSDA, the substantial agreement of the overall experimental and simulated IR spectra allows us to assign each of the sharp components to a family of carbynes characterized by a specific ligand. The most intense band peaked at 2127 cm^{-1} matches the computed frequency (2138 cm^{-1}) of the IR-α mode of the sp^2-terminated C_4 carbynes, marked with P_1 in Fig. 2. Its large intensity indicates that these short chains predominate in the carbyne population of the sample. Next, the structure at 2195 cm^{-1} is assigned to the overlapping IR-α modes of C_6, C_8, and C_{10} sp^2-terminated chains (reported in Fig. 2 as P_2, P_4, and P_5). We attribute the broad shoulder spanning the 1900–2100 cm^{-1} region to the overlap of weaker unresolved IR-β modes of sp^2-terminated C_n-carbynes, with an even number of atoms $n \geq 8$,[30,31] whose frequencies, contrary to the α modes, redshift as a function of the chain length. Finally, the IR-α modes of sp^3-terminated C_6 and C_8 (P_6 and P_7 frequencies computed at 2282 cm^{-1} and 2287 cm^{-1}, respectively) match the absorption peak at 2245 cm^{-1}. As demonstrated by means of Raman spectroscopy,[4] sp^3-terminated chains are a minority species in this type of *sp*-sp^2 material and hence the IR contribution of the polyyne-like C_4 (P_3 peak at 2211 cm^{-1}) is probably so small that it is hidden under the IR-α peak of more abundant C_6, C_8, and C_{10} sp^2-terminated chains.

On the basis of this assignment of the spectral features of our pristine *sp*-sp^2 sample, the effects of oxidation can be studied. IR spectra were acquired after the exposure of the sample to a He-O_2 mixture. These spectra are compared to the spectrum of the as-deposited sample in Fig. 1. The gas exposure induces significant changes in both the 1000–1600 cm^{-1} region and in the *sp* band. The increase of the component at 1550 cm^{-1} and the sharpening of the shoulder at 1200 cm^{-1} indicate a graphitization process, and are consistent with previous Raman measurements.[13] The intensity increase at 1730 cm^{-1}, where the stretching mode of the C=O functional group is situated, proves the partial oxidation of the sp^2 matrix.[32] The changes in the spectral region associated to carbynes are less obvious. Further insight can be gained through the comparison with theoretical results for the vibrational properties of mono-oxidized sp^2-terminated carbynes. Table II summarizes the predicted IR-active frequencies.

Note that, due to the loss of symmetry, all normal modes of the chains become to some degree both Raman and IR active, with different displacement patterns compared to those of the modes of centro-symmetric structures.[29] In particular, the ν_{CO} mode (ν_1) is characterized by a large stretching of the C=O bond and small displacements of the other bonds. The computed frequencies match the feature at 1730 cm^{-1}, which experiences the most relevant intensity increase after He-O_2 exposure, thus confirming the oxidation of *sp* carbon chains. However, the computed IR intensity of this mode in oxidized carbynes is not especially large. The intensity acquired by the 1730 cm^{-1} peak stems, therefore, most likely mainly from the formation of carbonyl (C=O) species as a result of the sp^2 matrix oxidation.[32] The detailed analysis of the difference spectrum, shown in Fig. 1(b), reveals that the reaction with oxygen suppresses mainly the low-frequency *sp*-carbon components, associated to longer and hence more reactive carbynes.[4,13,18,19] In contrast, a remarkable intensity increase, together with a weak blue shift, characterizes the component at 2127 cm^{-1}.

These findings are consistent with the theoretical results obtained by Moras *et al.*[18,19] regarding the reactivity of H-terminated carbynes with oxygen: during exposure, O_2 molecules cleave carbynes, leading to the formation of short, oxidized chains. This process leads to progressive shortening of the chains and emission of CO and/or CO_2 molecules. These exothermic reactions reduce the fraction of long carbynes in favor of shorter chains displaying higher vibrational frequencies. As a consequence, the peak at 2127 cm^{-1} blueshifts toward the most intense IR-active mode of the mono-oxidized sp^2-terminated C_4 and C_6 chains (predicted by simulation at 2129 and 2142 cm^{-1}, respectively, see Table II) and shows an intensity increase ascribable to the formation of new short oxygen-terminated chains through the cleavage of longer carbynes.

For what concerns sp^2-terminated carbynes, other IR-active modes mostly of C_4, C_6, and C_8 chains contribute to the spectrum (see Table II, and the IR intensities reported in the Appendix). These modes with a large C=O bond stretching component are all predicted near 2300 cm^{-1}, in good agreement with the experimental peak at 2245 cm^{-1}. Consistently

TABLE II. The computed IR-active vibrational modes of mono-oxidized carbynes anchored to a graphene nanoribbon (NR). A star marks the mode whose intensity is the largest for each species.

Carbyne	ν_1 (νCO) (cm^{-1})	ν_2 (cm^{-1})	ν_3 (cm^{-1})	ν_4 (cm^{-1})	ν_5 (cm^{-1})
NR-C_4-O	1730	2129	2293*	...	...
NR-C_6-O	1747	2081	2142	2304*	...
NR-C_8-O	1758	2036	2083	2181	2311*

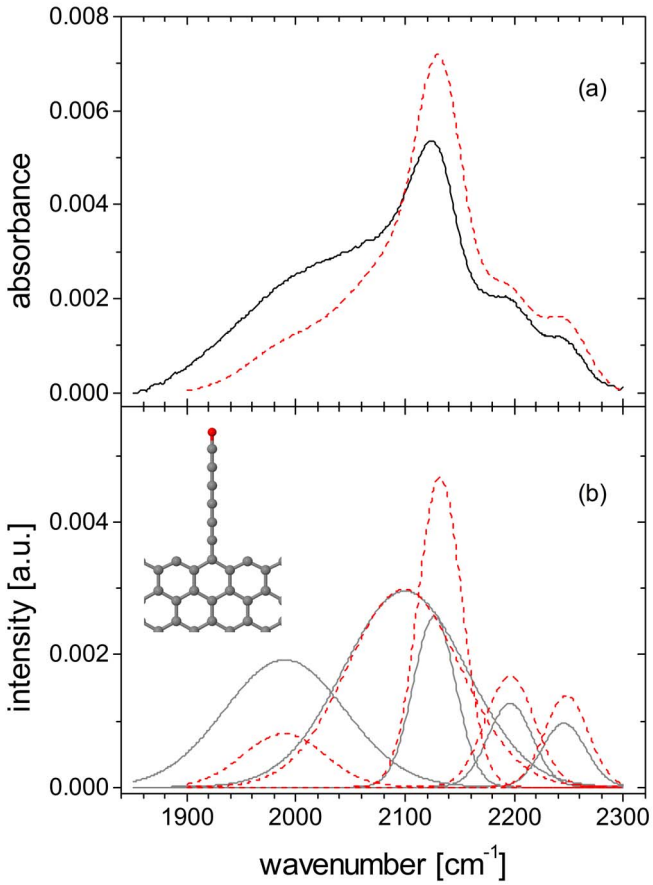

FIG. 3. (a) The IR spectra of the pure C sample before (solid line) and after exposure to 500 mbar of a He-O_2 mixture (dashed line). (b) Spectral decomposition as a sum of Gaussian peaks, as described in the Appendix. Solid: pristine (pure-C) sample; dashed: the same sample after exposure to a He-O_2 mixture. Inset: the simulation model for oxidized C_6 bonded to a graphene edge.

with this attribution, Fig. 3(b) shows that this peak also increases in intensity following He-O_2 exposure.

sp^3-terminated chains, whose IR-α modes also contribute (see Fig. 2) to this spectral region, represent a minority compared to sp^2 terminated ones and are less reactive to oxygen.[4] Indeed, the formation of oxidized sp^3-terminated chains is unlikely, as they would be characterized by bond-alternation frustration at the middle. Hence, few oxidized sp^3-terminated chains are expected to be embedded in the film.

Our experimental and theoretical results are, therefore, consistent with the following picture: the most relevant effect of He-O_2 exposure of a pure sp-sp^2 hybridized carbon film consists in the oxidation of both the sp^2 amorphous matrix and the sp^2-terminated carbynes. The final products are mostly short, end-oxidized carbynes anchored with a double bond to sp^2 fragments, plus an undetected amount of gaseous CO and/or CO_2.

IV. DISCUSSION AND CONCLUSION

In conclusion, by combining IR spectroscopy with *ab initio* calculations we studied the reactivity and oxidation of carbynes in a cluster-assembled sp-sp^2 pure-carbon film. This method can be applied for carbynes in any context, as long as no other strong vibrational peaks are present in the 1900–2300 cm^{-1} region. This identification of the spectral signatures of carbyne oxidation is of fundamental interest for the broad scientific community involved in the production and characterization of novel forms of carbon beyond graphene. Our results provide a crucial starting point for the design of carbyne-based nanoelectronic devices meant to operate outside UHV conditions.

Besides nanoelectronic applications, carbynes are also important in an astronomical context; carbon chain radicals have been detected in interstellar and circumstellar clouds, supporting the idea that they could play a role in the formation of more complex molecules in space. Our work provides fundamental data for astrophysics, namely, a quantitative input for the assessment of the concentration and evolution of pure-carbon species in the interstellar medium. Furthermore, by exposing the sp-sp^2 material to oxygen we identified the signatures of the formation of more stable oxidized chains. This study represents a potential breakthrough for the astrochemistry on carbon-based interstellar dust. It demonstrates that an active role of carbonaceous dust in producing CO or CO_2 has to be considered next to the traditional role of carbon clusters in atomic and molecular adsorption/desorption, surface-catalyzed chemical reactions among simple atoms/molecules (e.g., H, C, O, OH, CO) and energetic processing (by cosmic rays, X-rays, and UV radiation). Further studies will show how crucial this active role is in promoting more complex chemical species, essential for the formation of life such as amino acids.

ACKNOWLEDGMENTS

We thank the European Theoretical Spectroscopy Facility – ETSF[33] for support through the user Project No. 124.

APPENDIX: METHODS AND DATA ANALYSIS

The adopted software implementation of the DFPT cannot compute IR cross sections for metallic systems such as graphene nanoribbon ligands. To determine the IR intensities of the individual modes of the oxygen-terminated chains we performed the calculations of the vibrational spectra of carbynes with a $=CH_2$ group replacing the graphene nanoribbon termination. In such electronically gapped configurations we then determined the IR intensities, and in particular the most intense (designated as "α") IR-active mode for each carbyne length. We identified the vibrational bond-displacement pattern of CH_2-terminated chains, which most closely match the bond-displacement patterns for the modes of nanoribbon-terminated carbynes, as illustrated in Fig. 4. We then assigned the intensity computed for the CH_2-terminated chain to the best matching mode of the nanoribbon-terminated carbynes. The resulting IR cross sections are reported in Table III for carbynes of several lengths. It is apparent that longer chains exhibit a stronger IR activity.

The decomposition of the sp band was performed as follows: since the IR-α modes of carbynes C_n of different lengths

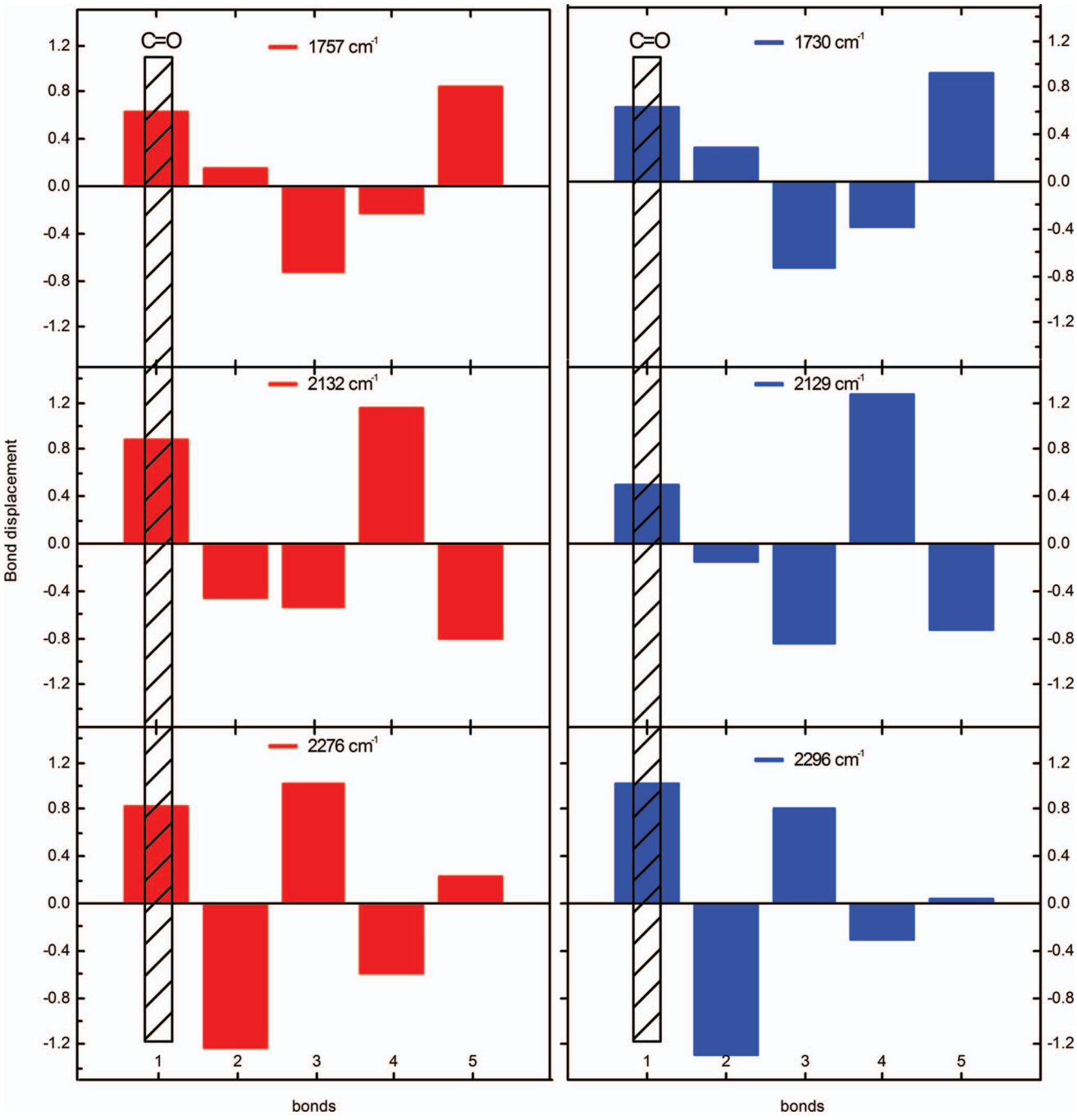

FIG. 4. Bond displacement patterns of the O-C4-CH2 (left panel) and the O-C4-NR (right panel) infrared-active vibrational modes. The displacement pattern is defined up to an arbitrary overall amplitude constant. In the calculation of the vibrational modes, the mass of H in the ligand is artificially fixed at 14 atomic mass units, to better simulate the mass of the graphitic fragment.

TABLE III. The computed frequencies of the mono-oxidized carbynes attached to a graphitic fragment: ν_1 is the frequency of the C=O functional group, ν_2-ν_5 are the stretching-mode frequencies of the chain. The IR intensities (in brackets) are evaluated for the indicated CH_2-terminated carbynes and reported in (D/A) ^{2}/amu units, where D is Debye, A is Angstrom, and amu is the atomic mass unit. The IR-α mode is highlighted by a star.

Compound	ν_1	ν_2	ν_3	ν_4	ν_5
CH_2-C_4-O	1797 (1.2)	2154 (0.4)	2299 (48.3)*	...	...
CH_2-C_6-O	1800 (1.8)	2092 (3.2)	2183 (11.6)	2293 (74.9)*	...
CH_2-C_8-O	1802 (1.1)	2046 (1.3)	2129 (40)	2189 (2.3)	2294 (97)*

cluster around the frequency imposed by the ligand geometry and do not disperse as a function of the carbyne length (up to $n = 10$), we fitted these sharp features with Gaussian peaks of a common width of ~45 cm^{-1}. More precisely, as the features at 2195 and 2245 cm^{-1} arise from the IR-α modes of sp^2- and sp^3-terminated ($n = 6, 8, 10$) chains, respectively, where we adopted slightly broader (48 cm^{-1}) Gaussians to represent these peaks. To represent the low-frequency components, containing an unresolved superposition of dispersing IR modes of carbynes longer than $n = 12$ plus the IR-α modes, we adopted broad Gaussians of width 130 cm^{-1}.

[1]M. Liu, V. I. Artyukhov, H. Lee, F. Xu, and B. I. Yakobson, ACS Nano **7**, 10075 (2013).
[2]B. Akdim and R. Pachter, ACS Nano **5**, 1769 (2011).
[3]O. Cretu, A. R. Botello-Mendez, I. Janowska, C. P. Huu, J.-C. Charlier, and F. Banhart, Nano Lett. **13**, 3487 (2013).
[4]L. Ravagnan, N. Manini, E. Cinquanta, G. Onida, D. Sangalli, C. Motta, M. Devetta, A. Bordoni, P. Piseri, and P. Milani, Phys. Rev. Lett. **102**, 245502 (2009).
[5]Y.-D. Guo, X.-H. Yan, and Y. Xiao, RSC Adv. **3**, 16672 (2013).
[6]Z. Zanolli, G. Onida, and J.-C. Charlier, ACS Nano **4**, 5174 (2010).
[7]M. G. Zeng, L. Shen, Y. Q. Cai, Z. D. Sha, and Y. P. Feng, Appl. Phys. Lett. **96**, 042104 (2010).
[8]W. Mohr, J. Stahl, F. Hampel, and J. A. Gladysz, Chem. Eur. J. **9**, 3324 (2003).
[9]X. Zhao, Y. Ando, Y. Liu, M. Jinno, and T. Suzuki, Phys. Rev. Lett. **90**, 187401 (2003).
[10]K. Inoue, R. Matsutani, T. Sanada, and K. Kojima, Carbon **48**, 4209 (2010).
[11]F. Cataldo, L. Ravagnan, E. Cinquanta, I. E. Castelli, N. Manini, G. Onida, and P. Milani, J. Phys. Chem. B **114**, 14834 (2010).
[12]L. Ravagnan, F. Siviero, C. Lenardi, P. Piseri, E. Barborini, and P. Milani, Phys. Rev. Lett. **89**, 285506 (2002).
[13]C. S. Casari, A. Li Bassi, L. Ravagnan, F. Siviero, C. Lenardi, P. Piseri, G. Bongiorno, C. E. Bottani, and P. Milani, Phys. Rev. B **69**, 075422 (2004).
[14]L. Ravagnan, T. Mazza, G. Bongiorno, M. Devetta, M. Amati, P. Milani, P. Piseri, M. Coreno, C. Lenardi, F. Evangelista, and P. Rudolf, Chem. Commun. **47**, 2952 (2011).
[15]W. A. Chalifoux and R. R. Tykwinski, Nature Chem. **2**, 967 (2010).
[16]C. Jin, H. Lan, L. Peng, K. Suenaga, and S. Iijima, Phys. Rev. Lett. **102**, 205501 (2009).
[17]A. Chuvilin, J. C. Meyer, G., Algara-Siller, and Ute Kaiser, New J. Phys. **11**, 083019 (2009).
[18]G. Moras, L. Pastewka, M. Walter, J. Schnagl, P. Gumbsch, and M. Moseler, J. Phys. Chem. C **115**, 24653 (2011).
[19]G. Moras, L. Pastewka, P. Gumbsch, and M. Moseler, Tribol. Lett. **44**, 355 (2011).
[20]W. W. Duley and A. Hu, Astrophys. J. **698**, 808 (2009).
[21]R. Papoular, Mon. Not. R. Astron. Soc. **434**, 862 (2013).
[22]S. Kwok and Y. Zhang, Nature (London) **479**, 80–83 (2011).
[23]M. Steglich, C. Jäger, F. Huisken, M. Friedrich, W. Plass, H.-J. Räder, K. Müllen, and T. Henning, Astrophys. J. Suppl. Ser. **208**, 26 (2013).
[24]E. Barborini, P. Piseri, and P. Milani, J. Phys. D: Appl. Phys. **32**, L105 (1999).
[25]K. Wegner, P. Piseri, H. Vahedi Tafreshi, and P. Milani, J. Phys. D: Appl. Phys. **39**, R439 (2006).
[26]P. Giannozzi *et al.*, J. Phys.: Condens. Matter **21**, 395502 (2009); open source code available at http://www.quantum-espresso.org.
[27]S. Baroni, S. de Gironcoli, A. Dal Corso, and P. Giannozzi, Rev. Mod. Phys. **73**, 515 (2001).
[28]A. C. Ferrari, S. E. Rodil, and J. Robertson, Phys. Rev. B **67**, 155306 (2003).
[29]R. A. Friedel and G. L. Carlson, J. Phys. Chem. **75**, 1149 (1971).
[30]E. Cinquanta, L. Ravagnan, I. E. Castelli, F. Cataldo, N. Manini, G. Onida, and P. Milani, J. Chem. Phys. **135**, 194501 (2011).
[31]N. R. Agarwal, A. Lucotti, D. Fazzi, M. Tommasini, C. Castiglioni, W. A. Chalifoux, and R. R. Tykwinski, J. Raman Spectrosc. **44**, 1398 (2013).
[32]M. Acik, G. Lee, C. Mattevi, A. Pirkle, R. M. Wallace, M. Chhowalla, K. Cho, and Y. Chabal, J. Phys. Chem. C **115**, 19761 (2011).
[33]A. Matsuura, N. Thrupp, X. Gonze, Y. Pouillon, G. Bruant, and G. Onida, Comput. Sci. Eng. **14**, 22 (2012).